THE JOURNAL OF PHYSICAL CHEMISTRY A

Article

pubs.acs.org/JPCA

Theoretical and Experimental Photoelectron Spectroscopy Characterization of the Ground State of Thymine Cation

Youssef Majdi

Laboratoire de Spectroscopie Atomique, Moléculaire et Applications (LSAMA), Université de Tunis El Manar, Tunis, Tunisia

Majdi Hochlaf*

Laboratoire Modélisation et Simulation Multi Echelle, MSME UMR 8208 CNRS, Université Paris-Est, 5 bd Descartes, 77454 Marne-la-Vallée, France

Yi Pan and Kai-Chung Lau*

Department of Biology and Chemistry, City University of Hong Kong, Kowloon, Hong Kong

Lionel Poisson

Laboratoire Francis Perrin, CNRS URA 2453, CEA, IRAMIS, Laboratoire Interactions Dynamique et Lasers, Bât 522, F-91191 Gif/Yvette, France

Gustavo A. Garcia and Laurent Nahon

Synchrotron SOLEIL, L'orme des Merisiers, Saint-Aubin, BP 48 91192 Gif-sur-Yvette Cedex France

Muneerah Mogren Al-Mogren

Chemistry Department, Faculty of Science, King Saud University, P.O. Box 2455, Riyadh 11451, Kingdom of Saudi Arabia

Martin Schwell

Laboratoire Interuniversitaire des Systèmes Atmosphériques (LISA), UMR 7583 CNRS, Universités Paris-Est Créteil et Paris Diderot, Institut Pierre et Simon Laplace, 61 Avenue du Général de Gaulle, 94010 Créteil, France

Supporting Information

ABSTRACT: We report on the vibronic structure of the ground state $\tilde{X}^2A''$ of the thymine cation, which has been measured using a threshold photoelectron photoion coincidence technique and vacuum ultraviolet synchrotron radiation. The threshold photoelectron spectrum, recorded over ~0.7 eV above the ionization potential (i.e., covering the whole ground state of the cation) shows rich vibrational structure that has been assigned with the help of calculated anharmonic modes of the ground electronic cation state at the PBE0/aug-cc-pVDZ level of theory. The adiabatic ionization energy has been experimentally determined as AIE = 8.913 ± 0.005 eV, in very good agreement with previous high resolution results. The corresponding theoretical value of AIE = 8.917 eV has been calculated in this work with the explicitly correlated method/basis set (R)CCSD(T)-F12/cc-pVTZ-F12, which validates the theoretical approach and benchmarks its accuracy for future studies of medium-sized biological molecules.

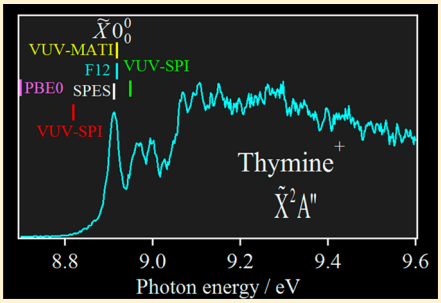

I. INTRODUCTION

Thymine (T) is a deoxyribonucleic acid (DNA) base of primary biological importance. The study of the mechanisms underlying the interaction of such compounds with ionizing light is crucial

Special Issue: Jean-Michel Mestdagh Festschrift

Received: October 25, 2014
Revised: December 23, 2014

DOI: 10.1021/jp510716c
J. Phys. Chem. A XXXX, XXX, XXX−XXX

to understand the damages produced by ionizing radiation on larger biomolecules, such as DNA and ribonucleic acid (RNA), and therefore, the hazardous genetic mutations potentially mediated by ions leading, for instance, to enhanced risk for cancer.[1−4] This requires a comprehensive understanding of their electronic structure and the accurate determination of their thermochemical data, such as their ionization energy (IE).

In this context, the vacuum ultraviolet (VUV) photoionization of thymine was studied by several groups. For instance, Lauer et al.,[5] Dougherty et al.,[6] Padva et al.,[7] and Urano et al.[8] measured the photoelectron spectra of thymine. The observed bands (rather large) were attributed to T^+ ionic electronic states. They were labeled according to the designation of orbitals from which they arise by the help of semiempirical computations. In 2005, Schwell and co-workers[9] performed a photoionization mass spectrometry study of thymine using BESSY I and BESSY II synchrotron radiation as excitation source in the 6−22 eV photon energy region. They found an experimental adiabatic ionization energy (AIE) of AIE = 8.82 ± 0.03 eV. One year later, the group at Daresbury Laboratory storage ring[10] presented an angularly resolved photoelectron spectrum of thymine. This spectrum was assigned using their computed binding energies (BEs) and spectral band intensities in the 8.82 to 17.35 eV energy range. These computations were done using outer-valence Green's function and algebraic-diagrammatic construction methods.[10] In addition, their angle-dependent photoelectron measurements helped to distinguish between σ and π orbitals in the assignment. For instance, these authors showed that the outermost molecular orbitals (MOs) of thymine have the following character and BE: $6a''(\pi_6)$, BE = 8.85 eV; $5a''(\pi_5)$, BE = 10.46 eV; $18a'$ $(\sigma_{LP\text{-}O})$, BE = 10.46 eV; $17a'(\sigma_{LP\text{-}O})$, BE = 11.36 eV; $4a''(\pi_4)$, BE = 12.52 eV. In general, these authors achieved a satisfactory agreement with their own and previous experimental spectra for the low-lying bands, whereas some of the inner-valence photoelectron bands, especially above 14 eV, are hard to assign because of the possible overlap between them.[10] More challenging, Choi et al.[11] measured a mass-analyzed threshold ionization (MATI) spectrum of thymine with a very high resolution (∼0.1 meV) in 2005. This spectrum corresponds to the photoionization of jet-cooled T close to the ionization threshold region, between its IE and IE + 1800 cm^{-1} (IE + 0.22 eV). It presents a rich structure that was attributed to the population of the lowest vibrational levels of the T^+ cation in its electronic ground state. This spectrum is dominated by the 0−0 transition, allowing one to accurately measure AIE(T) (= 8.9178 ± 0.0010 eV). The first normal-mode analysis of T^+ for the observed vibrational structure was also presented in the work of Choi et al.,[11] with the observed bands corresponding to the population of the low-frequency modes ν^+_{27}, ν^+_{30}, ν^+_{33}, and ν^+_{39} of T^+.

Later on, Bravaya et al.[12] presented a complete theoretical vibrational analysis of the T^+ (D_0) ground state between 8.7 and 9.7 eV. They used the high resolution MATI spectrum of Choi et al.[11] to satisfactorily test the quality of their calculations. They computed AIE(T) of 8.89 eV, which differs by only ∼0.02 eV from the AIE of Choi et al.[11] Also, the positions and relative intensities of the experimental vibrational bands were nicely reproduced by their (blue-shifted) theoretical spectrum. Moreover, these authors calculated the vertical ionization energies for the six lowest ionized electronic states of thymine using different theoretical methods. The ordering in energy of the electronic states and of their nature agree with the results of Trofimov et al.[10] and with those deduced from the experimental photoelectron spectrum (PES) band positions after differentiating their photoionization efficiency (PIE) spectrum (dPIE/dE curve).[12] Nevertheless, the relative spectral intensities of the experimental PES bands from Trofimov et al.[10] are not well-reproduced by the dPIE/dE curve.

More generally, previous theoretical and experimental works established that thymine, unlike other DNA bases (e.g., cytosine or guanine), has no low closely lying tautomers.[13] The most stable tautomer of thymine in the gas phase possesses a diketo structure,[14,15] while the most stable enolic tautomer lies ∼45 kJ/mol (∼0.47 eV) higher than that of the diketo tautomer.[13] Eleven other tautomers were also identified, with energies up to 130 kJ/mol above the most stable one. Therefore, the temperature needed to vaporize thymine, close to 500 K,[16] will produce a molecular jet with a unique tautomer associated with the diketo structure. The gas-phase PES spectrum is therefore not complicated by the contribution of several tautomers prior to ionization. However, the rotation of the methyl group of thymine (Figure 1) gives rise to two possible conformers, cis and trans. The trans form is a transition state. There is an interconversion barrier of ∼0.06 eV,[17] so that only the *cis*-rotamer is expected to be present in a jet-cooled molecular beam.

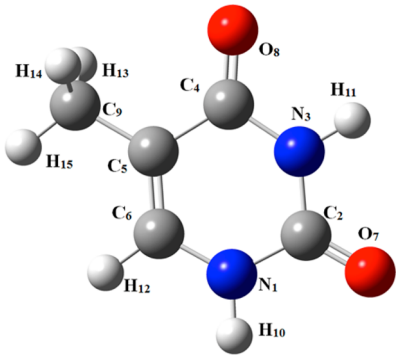

Figure 1. Numbering of the atoms constituting the thymine (neutral) molecule as used in the following tables.

To investigate the ionization process of thymine and explore the possible vibrational features of thymine cation, here we report a single photon ionization study of gas phase thymine by means of VUV synchrotron radiation coupled to a velocity map imaging electron/ion coincidence spectrometer. We recorded the slow photoelectron spectrum (SPES)[18−20] of thymine in the 8.7−9.7 eV range. Our work shows that the photoionization of T occurs mainly via a direct process near the ionization thresholds. The experimental spectra present rich vibrational structures from IE up to IE + 1 eV. These features correspond to the intact parent T^+ cation, since no fragmentation is expected below 10.7 eV as established by Schwell and co-workers.[9] We also performed ab initio computations for the determinations of the equilibrium geometry, the adiabatic ionization energy, and the harmonic and anharmonic frequencies of the T^+ cation ground state. With the help of these theoretical results, the experimental bands were attributed to the population of the vibrational levels of thymine$^+$ cation in its electronic ground state $(\tilde{X})$. This work extends, hence the previous investigations on this DNA basis, with the rich interplay offered by high level computations associated with the

DOI: 10.1021/jp510716c
J. Phys. Chem. A XXXX, XXX, XXX−XXX

SPES technique, combining quite high resolution and a broad binding energy range.

II. METHODOLOGIES

a. Theoretical Details. The geometry optimizations and derivation of harmonic and anharmonic frequencies of T and of T^+ in their electronic ground states are performed using the standard options as implemented in the GAUSSIAN09[21] and MOLPRO[22] suites of programs. All calculations were carried out in the C_1 point group.

These computations were done first using the pure functional of Perdew, Burke, and Ernzerhof with adiabatic connection functional model (PBE0)[23] and complete active-space self-consistent field (CASSCF)[24,25] method with aug-cc-pVDZ basis set.[26,27] In the PBE0 calculation, the spin contamination of T^+ is negligible as the eigenvalue of the S^2 operator is close to 0.75. The anharmonic frequencies at the PBE0/aug-cc-pVDZ level were obtained from the derivatives (second, third, and fourth) of the ground state potentials and second-order perturbation theory treatment of nuclear motions as implemented in GAUSSIAN09.[21] The CASSCF active space is constructed from the molecular orbitals HOMO−4 to LUMO+4, including the π and π^* orbitals of $C_2{=}O_7$, $C_4{=}O_8$, and $C_5{=}C_6$ bonds. The 9 core orbitals and the first 19 valence orbitals (up to HOMO−5) were kept as closed orbitals during the CASSCF calculations. This leads to 27720 configuration state functions (CSFs) to be treated.

In order to derive more accurate energetics with reduced computational cost, we performed computations at the (R)CCSD(T)-F12(b)/cc-pVTZ-F12 (+CV+SR+ZPVE) level as described in refs 28 and 29. Briefly, single-point calculations, at the geometries of T and T^+ optimized at PBE0/aug-cc-pVDZ level, are done using the (R)CCSD(T)-F12 (approximation b) explicitly correlated method[30−32] in connection with the cc-pVTZ-F12 explicitly correlated basis sets[33] and the corresponding auxiliary basis sets and density-fitting functions.[34−37] Then, we include the core−valence (CV, as the difference between CCSD(T)/cc-pwCVTZ[38,39] energies with and without considering core electrons) and scalar-relativistic (SR, as the difference between CCSD(T)/cc-pVTZ-DK[40−42] and CCSD(T)/cc-pVTZ energies) corrections. Finally, we took into account the zero-point vibrational energy correction (ZPVE) obtained at the PBE0 level.

b. Experimental Details. We performed electron/ion imaging coincidence spectroscopy on the VUV DESIRS beamline[43] at the third generation, French synchrotron facility SOLEIL located in St Aubin, France.

Thymine was placed into an in-vacuum stainless steel CF oven and heated to 200 °C. This temperature was chosen, since it is the minimum value to provide a satisfactory signal-to-noise ratio and, at the same time, ensuring the formation of a single thymine tautomer. Then, the resulting vapor was mixed with 1 bar of He and expanded through a 50 μm nozzle, which was situated at more than 2 cm from the skimmer to avoid clogging by deposition. Under these expansion conditions, no evidence of cluster formation was seen, either in the mass spectra or in the kinetic energy release distribution of the parent thymine ion. The skimmed molecular beam enters the ionization chamber where it crosses the synchrotron beam at a right angle. The electrons and ions produced were detected and mass and energy analyzed by the DELICIOUS III double imaging coincidence spectrometer.[44] The experimental setup and procedure to measure SPES spectra were already well-described in refs 18−20. In this study, the electrostatic conditions inside the ion source were such to ensure full transmission of photoelectrons with kinetic energies up to 3.5 eV. For the energy scans, the monochromator slit was set at 200 μm, giving a photon bandwidth of 12 meV at 10 eV. A pressure of 0.27 mbar of Ar was fed into the gas filter[45] to suppress high harmonics emitted by the undulator. Absorption lines of Ar in this filter are used to calibrate the energy scale to an absolute accuracy of better than 1 meV.

For each photon energy, the coincidence scheme yielded mass-filtered photoelectron images for all the species present in the mass spectrum. We monitored the ionization yield as well as the photoelectron spectra obtained with the pBasex algorithm[46] as a function of the wavelength, all of which were obtained simultaneously. The data were normalized by the photon flux measured using a dedicated photodiode (AXUV, IRD) placed downstream of the photon/sample interaction region.

III. RESULTS AND DISCUSSION

a. Equilibrium Geometries and Vibrational Spectroscopy of $T^+(\tilde{X}^2A'')$. Similar to the neutral molecule, the ground state is of cis structure (Figure 1), whereas the trans cationic form corresponds to a transition state. The ground state of T^+ cation is of the $\tilde{X}^2A''$ space symmetry. It is obtained by removal of one electron from the outermost a″ molecular orbital (π type) of thymine as given in ref 12. We give in Table 1 the main equilibrium geometrical parameters of neutral thymine and of its cation computed at the PBE0/aug-cc-pVDZ and CASSCF/aug-cc-pVDZ levels. To assess the accuracy of our results, we

Table 1. Main Geometrical Parameters (Angstroms and Degrees) of the Thymine Cation Ground State, Obtained at the PBE0/aug-cc-pVDZ and CASSCF/aug-cc-pVDZ Levels of theory

method	PBE0[a]	B3LYP[b]	CASSCF[a]
basis set	aug-cc-pVDZ	6-31G(d,p)	aug-cc-pVDZ
$N_1{-}C_2$	1.435	1.447	1.438
$C_2{-}N_3$	1.367	1.373	1.361
$N_3{-}C_4$	1.393	1.401	1.398
$C_4{-}C_5$	1.488	1.494	1.479
$C_5{-}C_6$	1.408	1.409	1.427
$C_6{-}N_1$	1.321	1.326	1.293
$C_2{-}O_7$	1.198	1.201	1.201
$C_4{-}O_8$	1.206	1.211	1.201
$C_5{-}C_9$	1.465	1.473	1.490
$N_1{-}H_{10}$	1.020	1.021	1.005
$N_{13}{-}H_{11}$	1.018	1.018	1.001
$C_6{-}H_{12}$	1.092	1.087	1.079
$C_9{-}H_{13}$	1.104	1.100	1.088
$C_9{-}H_{14}$	1.104	1.100	1.088
$C_9{-}H_{15}$	1.094	1.090	1.084
$N_1{-}C_2{-}N_3$	113.5	113.0	114.1
$C_2{-}N_3{-}C_4$	127.0	127.3	126.5
$N_3{-}C_4{-}C_5$	115.5	115.3	115.8
$C_4{-}C_5{-}C_6$	118.1	118.2	117.3
$C_5{-}C_6{-}N_1$	120.6	120.6	121.2
$N_3{-}C_2{-}O_7$	127.2	127.6	127.5
$N_3{-}C_4{-}O_8$	122.3	122.4	122.2
$C_4{-}C_5{-}C_9$	118.7	118.6	120.2

[a]This work. [b]ref 49.

DOI: 10.1021/jp510716c
J. Phys. Chem. A XXXX, XXX, XXX−XXX

Table 2. Harmonic and Anharmonic Frequencies (in Inverse Centimeters) of Ground State ($\tilde{X}^2A''$) of Thymine$^+$, Obtained at the PBE0/aug-cc-pVDZ Level of Theory[a]

	method	ωB97X-D[b]	PBE0[c]		CASSCF[c]		
	basis set	6-31+G(d,p)	aug-cc-pVDZ		aug-cc-pVDZ		
no.	symmetry	harmonic	harmonic	anharmonic	anharmonic[d]	exptl[e]	assignment
1	a′	3611	3574	3398	3449		ν NH
2	a′	3590	3551	3382	3414		ν NH
3	a′	3230	3222	3074	3049		ν CH
4	a′	3189	3191	3051	2980		ν CH
5	a′	3038	3020	2885	2884		ν CH
6	a′	1910	1857	1824	1737		$\nu(C_2O_7)$, β NH
7	a′	1813	1776	1723	1710		$\nu(C_4O_8)$, β NH
8	a′	1629	1615	1570	1608	1541	$\nu(C_6N_1)$, β CH
9	a′	1549	1540	1503	1508		β NH, δ ring
10	a′	1488	1453	1408	1447		β CH, δ ring
11	a′	1453	1433	1385	1400		β NH, δ ring
12	a′	1408	1407	1364	1392		β NH, δ ring
13	a′	1381	1350	1313	1362		β CH, δ ring
14	a′	1337	1315	1278	1293	1289	β CH, δ ring
15	a′	1300	1294	1260	1248	1244	β NH, δ ring
16	a′	1252	1236	1208	1219		β CH, δ ring
17	a′	1216	1208	1181	1155		δ ring, β NH
18	a′	1004	989	970	978		β NH, β CH
19	a′	919	917	898	901		β CH, δ ring
20	a′	777	778	761	742	730	δ ring, β CH
21	a′	710	716	701	676	688	δ ring, β CH
22	a′	587	582	577	556		δ ring, β CH
23	a′	537	533	525	518	523	δ ring, β CH
24	a′	447	444	440	431		δ ring, β CH
25	a′	396	391	387	374	389	$\delta(N_3C_2O_7)$, $\delta(N_3C_4O_8)$
26	a′	299	290	292	276		$\delta(C_4C_5C_9)$
27	a″	3095	3069	2899	2946		ω CH
28	a″	1434	1388	1336	1425		γ CH
29	a″	1012	1002	975	1033		γ CH
30	a″	954	939	910	972		γ CH
31	a″	780	799	782	775		γ NH, γ CH
32	a″	716	756	737	697		γ NH, τ ring
33	a″	687	707	685	647		γ NH, τ ring
34	a″	668	687	668	598		γ NH, τ ring
35	a″	379	391	383	375		γ CH, τ ring
36	a″	282	290	282	266		τ ring, γ CH
37	a″	136	145	140	118		τ ring
38	a″	102	107	104	94		τ ($-CH_3$ group)
39	a″	58	77	82	75	38	τ ($-CH_3$ group)

[a]Anharmonic frequencies are arranged according to the harmonic frequencies. The vibrational mode assignments are based on the PBE0 calculations. In-plane vibration: ν stretching, β bending, and δ deformation. Out-of-plane vibration: γ wagging, ω anti-symmetry stretching, and τ torsion. [b]Ref 12. [c]This work. [d]CASSCF/aug-cc-pVDZ harmonic frequencies scaled by 0.91. See ref 50. [e]Ref 11.

list in Table S1 of the Supporting Information the molecular parameters of neutral T ground state and their comparison to previous experimental and theoretical data. This table shows that the present PBE0/aug-cc-pVDZ data are in close agreement with those deduced from X-ray studies[47] and those computed using the costly CC2/TVZP method.[48] Accordingly, the PBE0s achieved accuracy is large enough for the present study. Particularly, for $T^+(\tilde{X}^2A'')$, Table 1 shows that both our PBE0/aug-cc-pVDZ and CASSCF/aug-cc-pVDZ structural parameters are in agreement with those deduced using B3LYP/6-31G(d,p) by Wetmore et al.[49]

Inspection of the geometrical parameters of both neutral and cationic species reveals that the main changes between $T(\tilde{X}^1A')$ and $T^+(\tilde{X}^2A'')$ occur for the bond lengths N_1-C_2 and C_5-C_6 together with slight changes for $C_5-C_6-N_1$, $N_1-C_2-O_7$, and $N_3-C_4-O_8$ in-plane angles. These geometrical changes should result in relatively long vibrational progressions for the population of some vibrational modes of the cation. Since vibrational analysis exists only for some $T^+(\tilde{X}^2A'')$ vibration modes,[11,12] we computed the harmonic and anharmonic frequencies of the $T^+(\tilde{X}^2A'')$ state. The corresponding results are given in Table 2. These frequencies are listed in a descending order under a′ symmetry (in-plane vibrations) and then a″ symmetry (out-of-plane vibrations). We present in Table S2 of Supporting Information the frequencies of neutral $T(\tilde{X}^1A')$ together with their comparison with previous theoretical and experimental works. Generally, our anharmonic frequencies differ by less than 20−30 cm^{-1} from the most

DOI: 10.1021/jp510716c
J. Phys. Chem. A XXXX, XXX, XXX−XXX

accurate determinations found in the literature. Such an accuracy is good enough for the assignment of the present vibrationally resolved experimental spectrum. In addition, we present in Table 2, the identification of these frequencies in terms of normal modes.

b. Presentation of the 2D and 1D SPES Spectra of T. The photoionization matrix of thymine in the photon energy range of 8.7−9.6 eV is presented in Figure 2a. This three-dimensional matrix represents the number of electron/ion coincidences (as a color code, ascending from black to blue) as a function of the photoelectron's kinetic energy and the photon energy. This spectrum presents several diagonal bright lines, which correspond to the vibrational cationic levels populated by direct ionization. The matrix reveals no obvious autoionization processes that would be resonant with the photon energy and thus would appear as localized spots in Figure 2a, aligned over discrete vertical lines, instead of diagonal lines. Then, as previously described (cf. refs 18−20), one can integrate the electron signal along the diagonal lines up to a certain kinetic energy to obtain the SPES, which yields a more favorable compromise between signal-to-noise and resolution than the commonly used TPES, where only threshold electrons with close-to-zero kinetic energy are considered. The resulting spectrum is given in Figure 2b. It exhibits a signal onset around 8.9 eV followed by rich well-resolved structures. This work extends the experimental spectrum of Choi et al.[11] limited to ~0.2 eV above the AIE, to cover the whole T^+ ($\tilde{X}^2A''$) band.

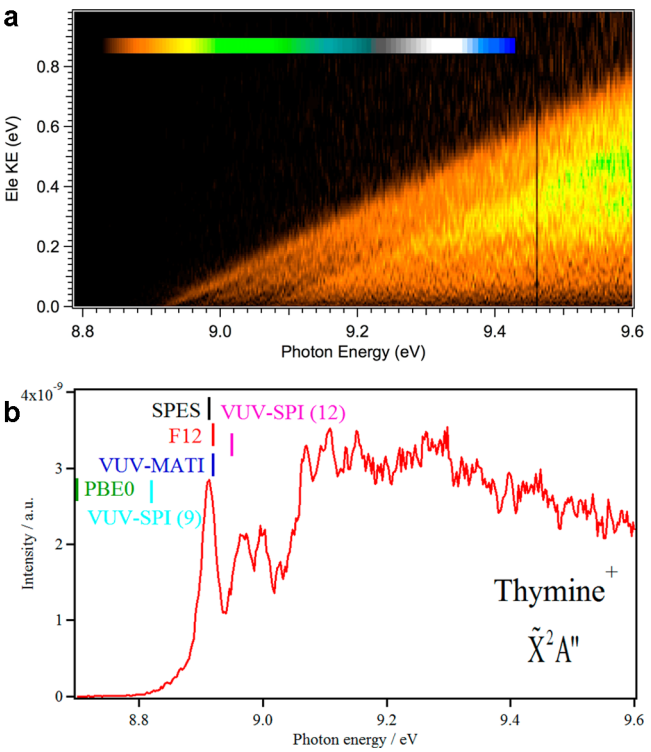

Figure 2. (a) 2D photoionization matrix of thymine providing the electron signal as a function of its kinetic energy and the photon energy. The photon energy step is 2.5 meV. (b) Slow photoelectron spectrum (SPES) deduced from the 2D spectrum after considering all electrons having kinetic energies between 0 and 70 meV. The total energy resolution is close to 30 meV. The vertical combs are for the present and previous determinations of AIE of thymine: this work at the PBE0/aug-cc-pVDZ (+ZPVE) (in green), at the (R)CCSD(T)-F12(b) (+CV+SR+ZPVE) (in red), and SPES (in black). VUV-MATI[11] (in blue), VUV-SPI (9)[9] (in light blue), and VUV-SPI (12)[12] (in pink).

c. Adiabatic Ionization Energy (AIE) of Thymine. The first intense vibrational band of the SPES spectrum at $h\nu$ = 8.913 ± 0.005 eV corresponds to the AIE of thymine [i.e., thymine ($\tilde{X}^1A'$) + $h\nu \rightarrow$ thymine$^+$ ($\tilde{X}^2A''$) + e^- photoionization transition], where both the neutral and the ion are in their vibrationless level. It is unlikely that this peak is due to hot bands because of the cooling of thymine within the molecular jet and its high intensity. Our value is in excellent agreement with the very accurate VUV-MATI AIE (= 8.9178 ± 0.0010 eV) of Choi et al.,[11] considering the given error bars in both methods. The (R)CCSD(T)-F12(b) (+CV+SR+ZPVE) calculated AIE (of 8.917 eV) shows also an outstanding agreement with these two experimental AIEs, especially with the VUV-MATI AIE. The high performance of this theoretical procedure was already noticed in ref 28.

Figure 2b shows graphically that other experimental methods, namely VUV-SPI in connection to mass spectrometry (sometimes called "PIMS" for photoionization mass spectrometry or "PIE" for photoionization efficiency measurements), and the theoretical PBE0 DFT methodologies fail to reach such accuracy for the AIE of such compounds. For instance, the discrepancy with the VUV-SPI IE value found by Jochims et al. (8.82 ± 0.03 eV)[9] is of the order of 0.1 eV too low. This is most reasonably explained by the initial thermal energy content of the thymine neutrals produced by the source used in ref 9. In addition, the pointing error is increased in VUV-SPI measurements since, contrary to methods where the electron energy is analyzed, they represent the integral of all the states lying below the photon energy. The VUV-SPI IE value of Bravaya et al. (8.95 ± 0.05 eV),[12] stated to correspond to the AIE by these authors, is too high by about 0.04 eV. This points to a low sensitivity for ion detection with their spectrometer in the threshold region where the ion formation quantum yield is low. Our current work highlights the interest of combining the SPES and the explicitly correlated theoretical methods for the determination of very accurate adiabatic ionization energies of medium-sized biologically relevant molecular species.

d. Tentative Assignment of the SPES Spectrum. Both the neutral and the cation belong to the C_s point group, vibrational excitation of a′ and even overtones of a″ vibrational modes are symmetry allowed upon single photon ionization. We propose in Figure 3 and Table 3 a tentative assignment of the vibrational photoelectron bands. These assignments are based on the anharmonic vibrational frequency predictions (Table 2), on the decomposition of the corresponding normal modes on the internal coordinates, and on the analysis of Bravaya et al.[12] The present experimental resolution does not allow resolving the low frequency modes (i.e., ν^+_{27}, ν^+_{30}, ν^+_{33}, and ν^+_{39}) observed by Choi et al.[11]

We fully assign these vibrational features to the pure vibrational progressions or combination modes involving the vibrational modes 7, 8, 10, 14, 15, 19, 20, 21, 23, 25, and 26. We measure hence ν^+_7 = 1750, ν^+_8 = 1548, ν^+_{10} = 1452, ν^+_{14} = 1282, ν^+_{15} = 1226, ν^+_{19} = 903, ν^+_{20} = 726, ν^+_{21} = 661, ν^+_{23} = 484, ν^+_{25} = 395, and ν^+_{26} = 258 (all values are in inverse centimeters). All these modes, for which Krylov and co-workers[12] predicted nonzero Franck−Condon transition intensities, are active upon single photoionization of neutral thymine. Nevertheless, our attribution presents some deviations from the one proposed by these authors. Indeed, we did reassign the peak at 9.093 eV to the $\tilde{X}10^1_0$ (computed at 1447

DOI: 10.1021/jp510716c
J. Phys. Chem. A XXXX, XXX, XXX−XXX

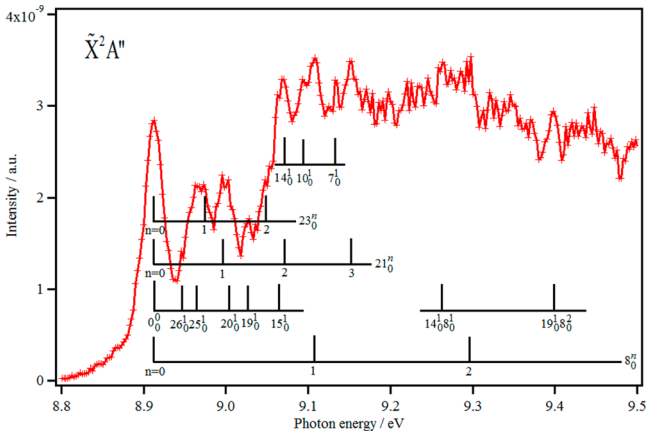

Figure 3. Tentative assignment (comb lines) of the SPES spectrum of $T^+(\tilde{X}^2A'')$. We considered all electrons having kinetic energies between 0 and 70 meV.

Table 3. Tentative Assignment for the Observed Frequencies of Photoionization Bands from the SPES Spectrum

tentative assignment	observed energy (eV)	observed frequencies[a] (cm^{-1})
$\tilde{X}0_0^0$	8.913	0
$\tilde{X}26_0^1$	8.945	258
$\tilde{X}25_0^1$	8.962	395
$\tilde{X}23_0^1$	8.973	484
$\tilde{X}21_0^1$	8.995	661
$\tilde{X}20_0^1$	9.003	726
$\tilde{X}19_0^1$	9.025	903
$\tilde{X}23_0^2$	9.045	1064
$\tilde{X}15_0^1$	9.065	1226
$\tilde{X}14_0^1$ or $\tilde{X}_0^2$	9.072	1282
$\tilde{X}10_0^1$ or $\tilde{X}32_0^2$ or $\tilde{X}20_0^2$	9.093	1452
$\tilde{X}8_0^1$	9.105	1548
$\tilde{X}7_0^1$	9.130	1750
$\tilde{X}21_0^3$	9.150	1911
–		
$\tilde{X}14_0^1 8_0^1$	9.260	2798
–		
$\tilde{X}8_0^2$	9.295	3081
–		
$\tilde{X}19_0^1 8_0^2$	9.398	3912

[a]Relative to the origin band of thymine$^+$.

cm^{-1}, Table 2) transition instead of the $\tilde{X}12_0^1$ since the computed anharmonic frequency for mode 12 (of 1364−1392 cm^{-1}) is too low compared to the experimental one. This band may correspond also to the $\tilde{X}32_0^2$ or $\tilde{X}20_0^2$ transitions that are expected to lie there. For the band at 9.072 eV, we propose either the $\tilde{X}14_0^1$ transition or the $\tilde{X}21_0^2$ transition. For energies >9.2 eV, the SPES spectrum consists of unresolved bands because of the contribution of several transitions. Nevertheless, we propose the following attribution to the bands: $\tilde{X}14_0^1 8_0^1$ at 9.260 eV, $\tilde{X}8_0^2$ at 9.295 eV, and $\tilde{X}19_0^1 8_0^2$ at 9.398 eV. Note that we are quite confident in the assignments of the fundamentals since they correspond to isolated peaks in the experimental spectra, whereas the deduction may be tentative for the combination and overtones bands because of the congestion of the spectrum at these energies.

IV. CONCLUSIONS

We investigated the vibrational structure of the ground state of the thymine$^+$ cation using combined theoretical and experimental SPES approaches. The experimental spectrum presents rich vibrational structures that extend the earlier work of Choi et al.[11] using a VUV-MATI technique toward a full coverage of the cation ground state. Taking advantage of the optimized resolution/statistics offered by the SPES technique, we were able to determine the fundamentals and some overtones and combination modes involving the cationic vibrational modes 7, 8, 10, 14, 15, 19, 20, 21, 23, 25, and 26. We further demonstrated that the SPES techniques allow for accurate measurement of the AIE of better than 5 meV for such biological compounds. Generally, we found an excellent agreement between the present experimental and theoretical determinations and previous works.

■ ASSOCIATED CONTENT

Ⓢ Supporting Information

Full lists of coauthors for refs 18, 21, and 22 are provided. Main geometrical parameters and harmonic and anharmonic frequencies of the neutral thymine ground state computed presently and their comparison to previous works (Tables S1 and S2, respectively). This material is available free of charge via the Internet at http://pubs.acs.org.

■ AUTHOR INFORMATION

Corresponding Authors

*E-mail: hochlaf@univ-mlv.fr. Tel: +33160957319. Fax: +33160957320.

*E-mail: kaichung@cityu.edu.hk. Tel: +85234426849. Fax: +85234420522.

Notes

The authors declare no competing financial interest.

■ ACKNOWLEDGMENTS

This study was undertaken while M.H. was a Visiting Professor at King Saud University. The support of the Visiting Professor Program at King Saud University is hereby gratefully acknowledged. Y.M. and M.H. acknowledge Marie Curie International Research Staff Exchange Scheme Fellowship within the 7th European Community Framework Program under Grant PIRSES-GA-2012-31754 and COST ACTION CM1405 MOLIM. We would like to thank financial support from the French national research program, Physique et Chimie du Milieu Interstellaire (PCMI) (CNRS, CNES). Parts of the theoretical work were supported by the Research Grants Council of Hong Kong (CityU 101512). We are indebted to the general technical staff of Synchrotron Soleil for running the facility under project 20131221. We would also like to thank Jean-François Gil for his technical help on the SAPHIRS molecular beam chamber.

■ REFERENCES

(1) Hagen, U. Current Aspects on the Radiation Induced Base Damage in DNA. *Radiat. Environ. Biophys.* **1986**, *25*, 261−271.

(2) Kumar, A.; Sevilla, M. D. Proton-Coupled Electron Transfer in DNA on Formation of Radiation-Produced Ion Radicals. *Chem. Rev.* **2010**, *110*, 7002−7023.

(3) Shikazono, N.; Noguchi, M.; Fujii, K.; Urushibara, A.; Yokoya, A. The Yield, Processing, and Biological Consequences of Clustered DNA Damage Induced by Ionizing Radiation. *J. Radiat. Res.* **2009**, *50*, 27−36.

DOI: 10.1021/jp510716c
J. Phys. Chem. A XXXX, XXX, XXX−XXX

(4) Gómez-Tejedor, G. G.; Fuss, M. C. *Radiation Damage in Biomolecular Systems*. Springer: Dordrecht, 2012.
(5) Lauer, G.; Schäfer, W. W.; Schweig, A. Functional Subunits in the Nucleic Acid Bases Uracil and Thymine. *Tetrahedron Lett.* **1975**, *16*, 3939−3942.
(6) Dougherty, D.; Wittel, K.; Meeks, J.; McGlynn, S. P. Photoelectron Spectroscopy of Carbonyls. Ureas, Uracils, and Thymine. *J. Am. Chem. Soc.* **1976**, *98*, 3815−3820.
(7) Padva, A.; O'Donnell, T. J.; LeBreton, P. R. UV Photoelectron Studies of Biological Pyrimidines: The Valence Electronic Structure of Methyl Substituted Uracils. *Chem. Phys. Lett.* **1976**, *41*, 278−282.
(8) Urano, S.; Yang, X.; LeBreton, P. R. UV Photoelectron and Quantum Mechanical Characterization of DNA and RNA Bases: Valence Electronic Structures of Adenine, 1,9-Dimethyl-guanine, 1-Methylcytosine, Thymine and Uracil. *J. Mol. Struct.* **1989**, *214*, 315−328.
(9) Jochims, H. W.; Schwell, M.; Baumgärtel, H.; Leach, S. Photoion Mass Spectrometry of Adenine, Thymine and Uracil in the 6−22 eV Photon Energy Range. *Chem. Phys.* **2005**, *314*, 263−282.
(10) Trofimov, A. B.; Schirmer, J.; Kobychev, V. B.; Potts, A. W.; Holland, D. M. P.; Karlsson, L. Photoelectron Spectra of the Nucleobases Cytosine, Thymine and Adenine. *J. Phys. B: At. Mol. Opt. Phys.* **2006**, *39*, 305−329.
(11) Choi, K. W.; Lee, J. H.; Kim, S. K. Ionization Spectroscopy of a DNA Base: Vacuum-Ultraviolet Mass-Analyzed Threshold Ionization Spectroscopy of Jet-Cooled Thymine. *J. Am. Chem. Soc.* **2005**, *127*, 15674−15675.
(12) Bravaya, K. B.; Kostko, O.; Dolgikh, S.; Landau, A.; Ahmed, M.; Krylov, A. I. Electronic Structure and Spectroscopy of Nucleic Acid Bases: Ionization Energies, Ionization-Induced Structural Changes, and Photoelectron Spectra. *J. Phys. Chem. A* **2010**, *114*, 12305−12317.
(13) Rejnek, J.; Hanus, M.; Kabeláč, M.; Ryjáček, F.; Hobza, P. Correlated *ab initio* Study of Nucleic Acid Bases and Their Tautomers in the Gas Phase, in a Microhydrated Environment and in Aqueous Solution. Part 4. Uracil and Thymine. *Phys. Chem. Chem. Phys.* **2005**, *7*, 2006−2017.
(14) Colarusso, P.; Zhang, K. Q.; Guo, B.; Bernath, P. F. The Infrared Spectra of Uracil, Thymine, and Adenine in the Gas Phase. *Chem. Phys. Lett.* **1997**, *269*, 39−48.
(15) Brown, R. D.; Godfrey, P. D.; McNaughton, D.; Pierlot, A. P. Microwave Spectrum of the Major Gas-phase Tautomer of Thymine. *J. Chem. Soc., Chem. Commun.* **1989**, *1*, 37−38.
(16) Ferro, D.; Bencivenni, L.; Teghil, R.; Mastromarino, R. Vapour Pressures and Sublimation Enthalpies of Thymine and Cytosine. *Thermochim. Acta* **1980**, *42*, 75−83.
(17) Dolgounitcheva, O.; Zakrzewski, V. G.; Ortiz, J. V. Ionization Energies and Dyson Orbitals of Thymine and Other Methylated Uracils. *J. Phys. Chem. A* **2002**, *106*, 8411−8416.
(18) Poully, J. C.; Schermann, J. P.; Nieuwjaer, N.; Lecomte, F.; Grégoire, G.; Desfrançois, C.; Garcia, G. A.; Nahon, L.; Nandi, D.; Poisson, L.; et al. Photoionization of 2-Pyridone and 2-Hydroxypyridine. *Phys. Chem. Chem. Phys.* **2010**, *12*, 3566−3572.
(19) Mahjoub, A.; Hochlaf, M.; Poisson, L.; Nieuwjaer, N.; Lecomte, F.; Schermann, J. P.; Grégoire, G.; Manil, B.; Garcia, G. A.; Nahon, L. Slow Photoelectron Spectroscopy of δ-Valerolactam and Its Dimer. *ChemPhysChem* **2011**, *12*, 1822−1832.
(20) Briant, M.; Poisson, L.; Hochlaf, M.; de Pujo, P.; Gaveau, M.-A.; Soep, B. Ar_2 Photoelectron Spectroscopy Mediated by Autoionizing States. *Phys. Rev. Lett.* **2012**, *109*, 193401−193405.
(21) Frisch, M. J.; Trucks, G. W.; Schlegel, H. B.; Scuseria, G. E.; Robb, M. A.; Cheeseman, J. R.; Scalmani, G.; Barone, V.; Mennucci, B.; Petersson, G. A. et al. *Gaussian 09*, revision A.02; Gaussian, Inc.; Wallingford, CT, 2009.
(22) Werner, H.-J.; Knowles, P. J.; Knizia, G.; Manby, F. R.; Schütz, M.; Celani, P.; Korona, T.; Lindh, R.; Mitrushenkov, A.; Rauhut, G. et al. *MOLPRO, ab initio programs package* (http://www.molpro.net), 2012.
(23) Adamo, C.; Barone, V. Toward Reliable Density Functional Methods Without Adjustable Parameters: The PBE0Model. *J. Chem. Phys.* **1999**, *110*, 6158−6170.
(24) Knowles, P. J.; Werner, H.-J. An Efficient Second-order MC SCF Method for Long Configuration Expansions. *Chem. Phys. Lett.* **1985**, *115*, 259−267.
(25) Werner, H.-J.; Knowles, P. J. A Second Order Multiconfiguration SCF Procedure with Optimum Convergence. *J. Chem. Phys.* **1985**, *82*, 5053−5063.
(26) Dunning, T. H. Gaussian Basis Sets for Use in Correlated Molecular Calculations. I. The Atoms Boron through Neon and Hydrogen. *J. Chem. Phys.* **1989**, *90*, 1007−1023.
(27) Kendall, R. A.; Dunning, T. H.; Harrison, R. J. Electron Affinities of the First-Row Atoms Revisited. Systematic Basis Sets and Wave Functions. *J. Chem. Phys.* **1992**, *96*, 6796−6806.
(28) Pan, Y.; Lau, K.-C.; Poisson, L.; Garcia, G. A.; Nahon, L.; Hochlaf, M. Slow Photoelectron Spectroscopy of 3-Hydroxyisoquinoline. *J. Phys. Chem. A* **2013**, *117*, 8095−8102.
(29) Pan, Y.; Lau, K.-C.; Al-Mogren, M. M.; Mahjoub, A.; Hochlaf, M. Theoretical Studies of 2-Quinolinol: Geometries, Vibrational Frequencies, Isomerization, Tautomerism, and Excited States. *Chem. Phys. Lett.* **2014**, *613*, 29−33.
(30) Adler, T. B.; Knizia, G.; Werner, H.-J. A Simple and Efficient CCSD(T)-F12 Approximation. *J. Chem. Phys.* **2007**, *127*, 221106.
(31) Werner, H.-J.; Knizia, G.; Manby, F. R. Explicitly Correlated Coupled Cluster Methods with Pair-specific Geminals. *Mol. Phys.* **2011**, *109*, 407−417.
(32) Knizia, G.; Adler, T. B.; Werner, H.-J. Simplified CCSD(T)-F12 Methods: Theory and Benchmarks. *J. Chem. Phys.* **2009**, *130*, 054104.
(33) Peterson, K. A.; Adler, T. B.; Werner, H.-J. Systematically Convergent Basis Sets for Explicitly Correlated Wavefunctions: The Atoms H, He, B−Ne, and Al−Ar. *J. Chem. Phys.* **2008**, *128*, 084102.
(34) Weigend, F. A Fully Direct RI-HF Algorithm: Implementation, Optimised Auxiliary Basis Sets, Demonstration of Accuracy and Efficiency. *Phys. Chem. Chem. Phys.* **2002**, *4*, 4285−4291.
(35) Hättig, C. Optimization of Auxiliary Basis Sets for RI-MP2 and RI-CC2 Calculations: Core−valence and Quintuple-ζ Basis Sets for H to Ar and QZVPP Basis Sets for Li to Kr. *Phys. Chem. Chem. Phys.* **2005**, *7*, 59−66.
(36) Klopper, W. Highly Accurate Coupled-Cluster Singlet and Triplet Pair Energies from Explicitly Correlated Calculations in Comparison with Extrapolation Techniques. *Mol. Phys.* **2001**, *99*, 481−507.
(37) Yousaf, K. E.; Peterson, K. A. Optimized Auxiliary Basis Sets for Explicitly Correlated Methods. *J. Chem. Phys.* **2008**, *129*, 184108.
(38) Watts, J. D.; Gauss, J.; Bartlett, R. J. Coupled-Cluster Methods with Noniterative Triple Excitations for Restricted Open-Shell Hartree−Fock and other General Single Determinant Reference Functions. Energies and Analytical Gradients. *J. Chem. Phys.* **1993**, *98*, 8718−8733.
(39) Peterson, K. A.; Dunning, T. H. Accurate Correlation Consistent Basis Sets for Molecular Core−valence Correlation Effects: The Second Row Atoms Al−Ar, and the First Row Atoms B−Ne Revisited. *J. Chem. Phys.* **2002**, *117*, 10548−10560.
(40) Douglas, M.; Kroll, N. M. Quantum Electrodynamical Corrections to the Fine Structure of Helium. *Ann. Phys.* **1974**, *82*, 89−155.
(41) Jansen, G.; Hess, B. A. Revision of the Douglas-Kroll Transformation. *Phys. Rev. A* **1989**, *39*, 6016−6017.
(42) de Jong, W. A.; Harrison, R. J.; Dixon, D. A. Parallel Douglas−Kroll Energy and Gradients in NWChem: Estimating Scalar Relativistic Effects using Douglas−Kroll Contracted Basis Sets. *J. Chem. Phys.* **2001**, *114*, 48−53.
(43) Nahon, L.; de Oliveira, N.; Garcia, G. A.; Gil, J.-F.; Pilette, B.; Marcouillé, O.; Lagarde, B. Polack, F. DESIRS: A State-of-the-Art VUV Beamline Featuring High Resolution and Variable Polarization for Spectroscopy and Dichroism at SOLEIL. *J. Synchrotron Radiat.* **2012**, *19*, 508−520.

DOI: 10.1021/jp510716c
J. Phys. Chem. A XXXX, XXX, XXX−XXX

(44) Garcia, G. A.; de Miranda, B. K. C.; Tia, M.; Daly, S.; Nahon, L. DELICIOUS III: A Multipurpose Double Imaging Particle Coincidence Spectrometer for Gas Phase Vacuum Ultraviolet Photodynamics Studies. *Rev. Sci. Instrum.* **2013**, *84*, 053112.
(45) Mercier, B.; Compin, M.; Prevost, C.; Bellec, G.; Thissen, R.; Dutuit, O.; Nahon, L. Experimental and Theoretical Study of a Differentially Pumped Absorption Gas Cell Used as a Low Energy-pass Filter in the Vacuum Ultraviolet Photon Energy Range. *J. Vac. Sci. Technol., A* **2000**, *18*, 2533−2541.
(46) Garcia, G. A.; Nahon, L.; Powis, I. Two-Dimensional Charged Particle Image Inversion Using a Polar Basis Function Expansion. *Rev. Sci. Instrum.* **2004**, *75*, 4989−4996.
(47) Stewart, R. F.; Jensen, L. H. Redetermination of the Crystal Structure of Uracil. *Acta Crystallogr.* **1967**, *23*, 1102−1105.
(48) Etinski, M.; Fleig, T.; Marian, C. M. Intersystem Crossing and Characterization of Dark States in the Pyrimidine Nucleobases Uracil, Thymine, and 1-Methylthymine. *J. Phys. Chem. A* **2009**, *113*, 11809−11816.
(49) Wetmore, S. D.; Boyd, R. J.; Eriksson, L. A. Radiation Products of Thymine, 1-Methylthymine, and Uracil Investigated by Density Functional Theory. *J. Phys. Chem. B* **1998**, *102*, 5369−5377.
(50) Gagliardi, L.; Orlandi, G.; Bernardi, F.; Cembran, A.; Garavelli, M. A Theoretical Study of the Lowest Electronic States of Azobenzene: The Role of Torsion Coordinate in the Cis−Trans Photoisomerization. *Theor. Chem. Acc.* **2004**, *111*, 363−372.

DOI: 10.1021/jp510716c
J. Phys. Chem. A XXXX, XXX, XXX−XXX